



# Utility of Penman–Monteith, Priestley–Taylor, reference evapotranspiration, and pan evaporation methods to estimate pasture evapotranspiration

David M. Sumner<sup>a,\*</sup>, Jennifer M. Jacobs<sup>b,1</sup>

<sup>a</sup>United States Geological Survey, 224 West Central Parkway, Suite 1006, Altamonte Springs, FL 32714, USA

<sup>b</sup>Department of Civil Engineering, University of New Hampshire, Durham, NH 03824, USA

Received 25 August 2003; revised 6 October 2004; accepted 29 October 2004

## Abstract

Actual evapotranspiration ( $ET_a$ ) was measured at 30-min resolution over a 19-month period (September 28, 2000–April 23, 2002) from a nonirrigated pasture site in Florida, USA, using eddy correlation methods. The relative magnitude of measured  $ET_a$  (about 66% of long-term annual precipitation at the study site) indicates the importance of accurate  $ET_a$  estimates for water resources planning. The time and cost associated with direct measurements of  $ET_a$  and the rarity of historical measurements of  $ET_a$  make the use of methods relying on more easily obtainable data desirable. Several such methods (Penman–Monteith (PM), modified Priestley–Taylor (PT), reference evapotranspiration ( $ET_0$ ), and pan evaporation ( $E_p$ )) were related to measured  $ET_a$  using regression methods to estimate PM bulk surface conductance, PT  $\alpha$ ,  $ET_0$  vegetation coefficient, and  $E_p$  pan coefficient. The PT method, where the PT  $\alpha$  is a function of green-leaf area index (LAI) and solar radiation, provided the best relation with  $ET_a$  (standard error (SE) for daily  $ET_a$  of 0.11 mm). The PM method, in which the bulk surface conductance was a function of net radiation and vapor-pressure deficit, was slightly less effective (SE = 0.15 mm) than the PT method. Vegetation coefficients for the  $ET_0$  method (SE = 0.29 mm) were found to be a simple function of LAI. Pan coefficients for the  $E_p$  method (SE = 0.40 mm) were found to be a function of LAI and  $E_p$ . Historical or future meteorological, LAI, and pan evaporation data from the study site could be used, along with the relations developed within this study, to provide estimates of  $ET_a$  in the absence of direct measurements of  $ET_a$ . Additionally, relations among PM, PT, and  $ET_0$  methods and  $ET_a$  can provide estimates of  $ET_a$  in other, environmentally similar, pasture settings for which meteorological and LAI data can be obtained or estimated.

© 2004 Elsevier B.V. All rights reserved.

**Keywords:** Evapotranspiration; Reference evapotranspiration; Pan evaporation; Pasture

## 1. Introduction

Quantification of actual evapotranspiration ( $ET_a$ ) is critical to water resources management because of the large share of the water budget typically composed of  $ET_a$ . Baumgartner and Reichel (1975) noted that

\* Corresponding author. Tel.: +1 407 865 6725x133.

E-mail address: [dmsummer@usgs.gov](mailto:dmsummer@usgs.gov) (D.M. Sumner).

<sup>1</sup> Tel.: +1 603 862 0635; fax: +1 603 862 3957.

worldwide,  $ET_a$  returns about 64% of land-based precipitation to the atmosphere. In Florida, the fraction of annual precipitation returned as ET ranges from about 50% in settings of relatively deep water-table, shallow rooted vegetation, and sandy soils (Sumner, 1996) to almost 110% from lakes (Swancar et al., 2000).

Water resources planning often requires the use of hydrologic models (usually numerical) to assess the impact (e.g. reduction in streamflows, wetland dehydration, or salt-water intrusion into an aquifer) of possible stresses (e.g. increased groundwater withdrawals associated with population growth) to a hydrologic system. Hydrologic models require spatial and temporal quantification of fluxes of water into, out of, and within the hydrologic system; the prominence of the outgoing flux of  $ET_a$  within the water budget dictates this flux must be estimated in most hydrologic models. It is interesting to note that it is the difference of precipitation and  $ET_a$  that provides the 'available water' to a hydrologic system for recharge to subsurface aquifers and stream flow and, as with any difference of two numbers (particularly if the two numbers are of comparable magnitude), relative error in precipitation or  $ET_a$  can be amplified within an estimate of available water, further supporting the need for the best estimates of  $ET_a$ .

Hydrologic models usually are 'calibrated' to measured historical data (e.g. water levels, flows, or constituent concentrations) to identify unknown model parameters and assess model performance. Spatial and temporal distributions of historical  $ET_a$  data are needed for such calibration simulations. However, direct measurements of  $ET_a$  are rarely available. For settings in which moisture is readily available (e.g. irrigated crops or open-water surfaces),  $ET_a$  is often estimated based on values of Penman–Monteith reference evapotranspiration ( $ET_0$ ) or pan evaporation ( $E_p$ ) and empirically derived correction factors (vegetation (or crop) and pan coefficients, respectively).  $ET_0$  (Allen et al., 1998; Walter et al., 2000) is the ET from a hypothetical, well-watered 'reference' crop.  $E_p$  (Kohler et al., 1955; Farnsworth et al., 1982) is the evaporation from an evaporation pan. However, estimating  $ET_a$  in moisture-stressed settings (e.g. wildlands or nonirrigated pasture) is more difficult and  $ET_a$  is usually inferred through use of a parameterized  $ET_a$  sub-model of the hydrologic

model. The  $ET_a$  sub-models within MODFLOW-2000, a widely used model for simulation of groundwater flow (Harbaugh et al., 2000), the MIKESHE watershed model (Danish Hydraulic Institute, 1998), and the HEC-HMS (US Army Corps of Engineers, 2000) watershed model each have unique parameterized approaches to estimating  $ET_a$  from a user-specified potential  $ET_a$  (maximum  $ET_a$  for a given surface if moisture is not limiting) and some indicator of moisture availability (e.g. water-table depth or soil moisture). The parameters within the  $ET_a$  sub-model generally are defined based on literature values or inferred through calibration of the hydrologic model. However, the literature-derived estimates of  $ET_a$  sub-model parameters generally are crude and the large number of unknown parameters within most hydrologic models often prevents a unique, calibration-derived identification of model parameters (including  $ET_a$  sub-model parameters). The parameter uncertainty in most hydrologic models degrades the utility of models for water resources planning.

Direct measurement of  $ET_a$  (e.g. by eddy correlation methods) provides an opportunity to improve the quality of hydrologic model calibration through reduction in the uncertainty of the  $ET_a$  component of the model in one of two ways: (1) prescribing the  $ET_a$  input in the model to the measured values or (2) comparison of the  $ET_a$  values inferred through the  $ET_a$  sub-model with the measured values, followed by refinement of the conceptualization or parameterization of the evapotranspiration sub-model. The rarity and expense of direct measurements of  $ET_a$  limits the utility of this approach. However, development of quantitative relations between  $ET_a$  and other indicators or models of  $ET_a$  that rely on easily obtainable data, offers the potential to estimate  $ET_a$  for improvement of hydrologic models. Such indicators or models of  $ET_a$  might include, (in order of increasing data requirements):  $E_p$  (requires measurement of daily evaporation from evaporation pan),  $ET_0$  (requires measurement of incoming solar radiation, air temperature, relative humidity, and wind speed), modified Priestley–Taylor equation (PT) (requires measurement of net radiation, soil heat flux, air temperature, and other environment-specific variables), and Penman–Monteith equation (PM) (requires measurement of net radiation, soil heat flux, air temperature, relative humidity, wind speed,

and other environment-specific variables). Although the utility of  $E_p$  and  $ET_0$  as indicators of  $ET_a$  from open water or well-watered settings is well established, the effectiveness of these methods and the form of the pan and vegetation coefficients in moisture-stressed settings has been less explored.

The PM equation (Monteith, 1965), a theoretically based ‘combination’ approach that incorporates energy and aerodynamic considerations, has been commonly used for plant canopies having adequate fetch and a canopy distribution sufficient to satisfy the ‘big-leaf’ assumption that the sources of sensible and latent heat are at the same height and temperature. The modified PT energy-based approach (Flint and Childs, 1991) is a simplification of the PM equation. Stannard (1993) noted that the PT approach was superior to the PM approach for a sparsely vegetated site in the semi-arid rangeland of Colorado. Likewise, Sumner (1996) noted the superiority of the PT approach for a site of herbaceous, successional vegetation in central Florida.

The PM and PT equations produce direct estimates of  $ET_a$ , but require knowledge of the PM canopy resistance or the PT  $\alpha$ , respectively. Many studies have indicated the site-uniqueness of canopy resistance and  $\alpha$  and that these variables depend on a number of factors (Jarvis, 1976; Dolman et al., 1988; Stewart, 1988). These factors include leaf area index (Kustas et al., 1996), soil water availability (Parton et al., 1981; Wright et al., 1995), elevation (Rosset et al., 1997), soil characteristics, vapor-pressure deficit (Bidlake, 2002), and solar radiation (Wright et al., 1995). However, other studies have determined that one or more of the above factors had no influence on canopy resistance or  $\alpha$  (Stannard, 1993).

The primary objective of this paper is to suggest a possible method for using calibrated relations between  $ET_a$  (for the variety of land covers of interest to water managers) and less-expensive/more available proxies for  $ET_a$ . The pasture site chosen for this study is an areally significant land cover in the local area of interest (west-central Florida, USA). Pastures cover 9% of the contiguous United States (Vogelmann et al., 2001) and occur extensively throughout the world. In this paper, the utility of PM, PT,  $ET_0$ , and  $E_p$  methods to estimate  $ET_a$  from a site subject to moisture stress (nonirrigated pasture) was examined. Each of the methods was quantitatively related to eddy correlation measurements of  $ET_a$  collected during a 19-month

experiment (September 28, 2000–April 23, 2002). The PM and PT methods were compared at a 30-min resolution; all methods were compared at daily resolution.

## 2. Site description

The study was conducted within a commercial farm (Ferris Farms) near Floral City, Florida, USA. The farm is located on a sand ridge in west-central Florida bounded by residential areas, a lake, and wetlands (Fig. 1). This ridge is part of an extensive network of sand ridges in central Florida that are characterized by sandy soils, relatively deep water tables, and low surface runoff; these sand ridges are areas of relatively high recharge to the surficial aquifer system. Soils are fine sands (hyperthermic coated Typic Quartzipsamments). The water table was estimated to be 6–9 m below land surface, based on the altitude of the water surface in the nearby lake (about 12 m above sea level) and the range of land-surface altitudes at the study site (18–21 m). The climate of the area is humid subtropical and is characterized by a warm, wet season (June–September) and a mild, dry season (October–May). Rainfall averages about 1360 mm yr<sup>-1</sup> based on 52 years of record at a National Oceanographic and Atmospheric Administration (NOAA) weather station near the City of Inverness, about 10 km northwest of the study site. During the dry season, rainfall typically is associated with frontal systems and often is areally extensive. More than 50% of the annual rainfall generally occurs during the wet season, when localized convective thunderstorm activity is common. Fig. 2a–c shows the cumulative precipitation, average daily temperature, and average daily incoming solar radiation, respectively, at the study site. Mean air temperature is about 21 °C, ranging from occasional winter temperatures below 0 °C to summer temperatures approaching 35 °C. Incoming solar radiation at land surface generally peaks about a month before the start of summer because of increasing cloudiness in late spring and summer.

Land-surface vegetation near the study site includes pastures of Bahia grass (*Paspalum notatum* Flugge) and agricultural fields rotated between fields of strawberries (*Fragaria* sp.) and brown top millet (*Panicum ramosum*). The pastures are subject to

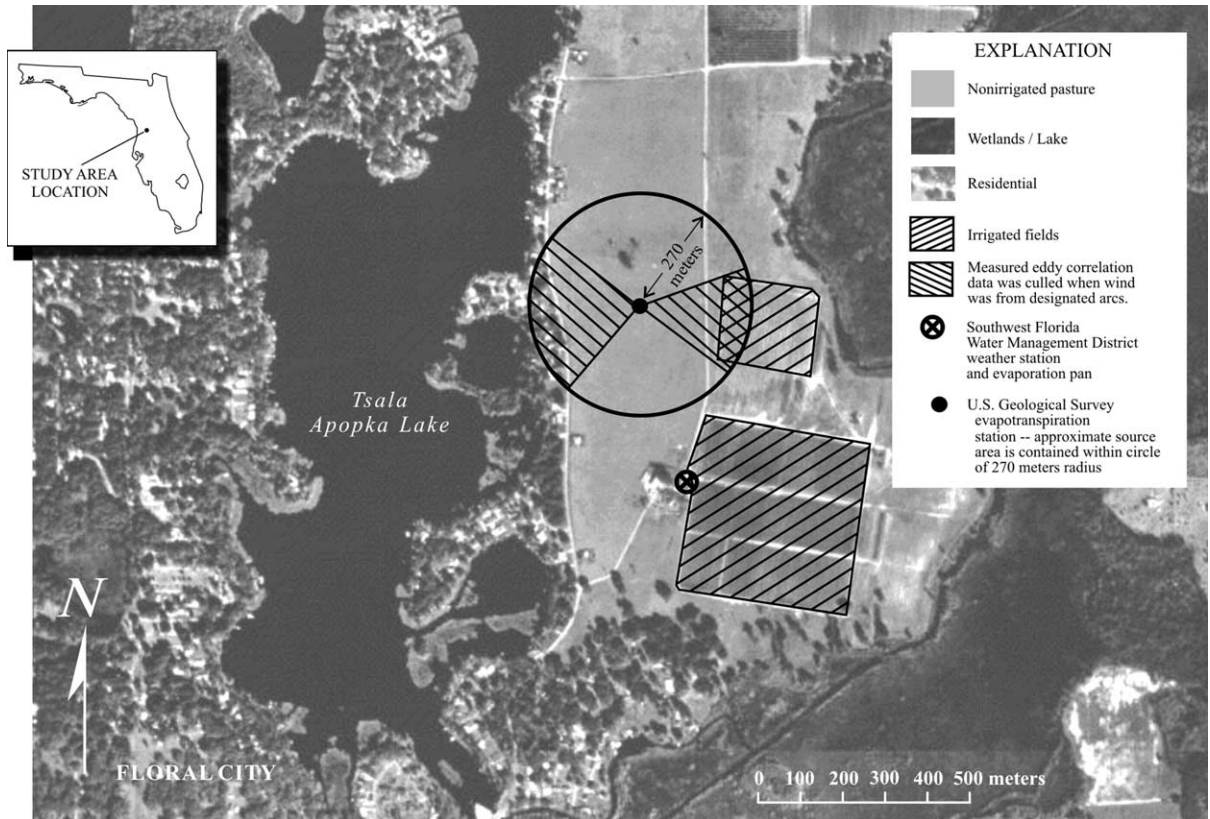


Fig. 1. Location of study area near Floral City, Florida, USA.

rotational grazing by cattle. The nonirrigated pastures vary from a lush green during the summer to a drab brown during the winter. Grass height averages about 8–12 cm. A seed head develops during the summer on a stalk that can reach 30 cm in height. Bahia grass rooting depth can exceed 2 m.

### 3. Field measurements

Continuous measurements were made at the study site (Fig. 1) from September 28, 2000, through April 23, 2002. The study site had two instrumented locations. Eddy correlation and ancillary sensors were located within the pasture area for the current study. A long-term weather station and an evaporation pan, both operated by the Southwest Florida Water Management District for the measurement of  $ET_0$  and  $E_p$ , were located between the pasture area and agricultural fields. Station instrumentation is detailed in Table 1.

#### 3.1. Eddy correlation measurements

The eddy correlation station was sited to measure  $ET_a$  from a nonirrigated pasture. Eddy correlation methods (Dyer, 1961; Tanner and Greene, 1989) rely on high-frequency (generally 5 Hz, or higher) measurements of fluctuations in wind speed, vapor density, and air temperature to infer fluxes of vapor and sensible heat. The eddy correlation sensors (three-dimensional sonic anemometer and krypton hygrometer) were monitored at 8 Hz; latent heat and sensible heat fluxes were computed at 30-min resolution. Estimates of vapor flux were corrected for temperature-induced fluctuations in air density (Webb et al., 1980) and for the sensitivity of the hygrometer to oxygen (Tanner and Greene, 1989). Sensible heat flux was corrected for the error introduced by measuring fluctuations in 'sonic' rather than actual air temperature (Schotanus et al., 1983).

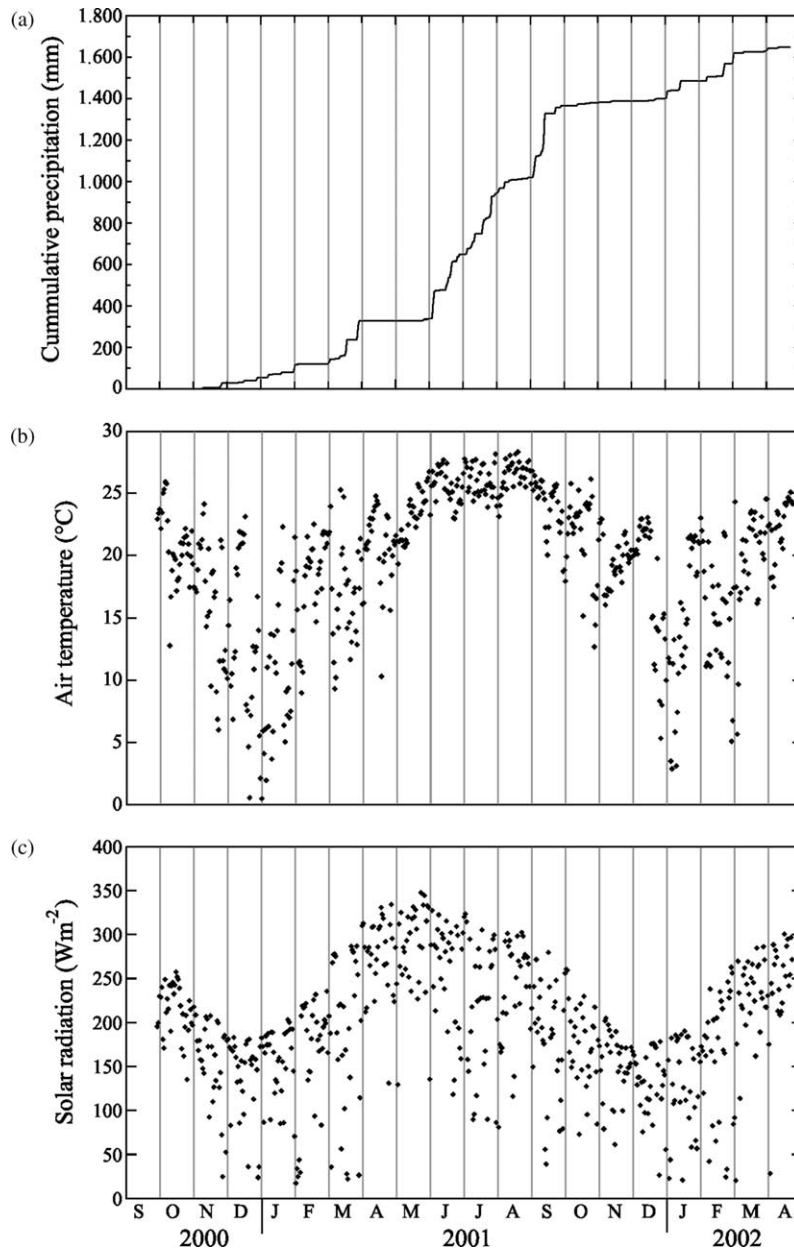


Fig. 2. Atmospheric parameters recorded during the study period: (a) cumulative precipitation, (b) daily average temperature values, and (c) daily average incoming solar radiation.

Any misalignment of the sonic anemometer with the airstream was corrected by the coordinate rotation procedure (Tanner and Thurtell, 1969; Baldocchi et al., 1988). Measurements for which the misalignment was greater than  $10^\circ$  were culled from the data.

Rainfall, dew, and scaling caused by exposure to the atmosphere may obscure the hygrometer windows, particularly in humid environments, and result in missing data. The problems associated with dew formation are particularly acute at night in humid

Table 1  
Study instrumentation

Type of measurement	Instrument <sup>a</sup>	Height(s) above land surface (m)
<i>SWFWMD weather station</i>		
Air temperature/relative humidity	CSI Model HMP45C temperature and relative humidity probe	1.8
Wind speed/direction	R.M. Young wind monitor Model 05103	2.9
Incoming solar radiation	LI-COR, Inc. Model LI200X pyranometer	2
Precipitation	Waterlog H-340	2.5
Pan evaporation	Class A evaporation pan	0.14
Datalogging	CSI Model 10X datalogger; 12-V deep-cycle battery; 20-W solar panel	0–1
<i>Eddy correlation station</i>		
Evapotranspiration	CSI eddy correlation system including Model CSAT3 three-dimensional sonic anemometer and Model KH20 krypton hygrometer	2.7
Air temperature/relative humidity	CSI Model HMP45C temperature and relative humidity probe	1.9
Net radiation	REBS Model Q-7.1 net radiometers (2)	2.7
Wind speed/direction	Handar Model 425 ultrasonic anemometer	3.3
Incoming solar radiation	LI-COR, Inc. Model LI200X pyranometer	2.8
Soil moisture	CSI Model CS615 water content reflectometer (2)	0 to –0.08 and 0 to –0.30
Soil temperature	CSI Model TCAV averaging soil thermocouple probes (2)	–0.02 and –0.06
Soil heat flux	CSI Model HFT-3 soil heat flux plates (2)	–0.08
Datalogging	CSI Model 10X dataloggers (2); 12-V deep-cycle batteries (2); 20-W solar panels (2)	0–1

CSI, Campbell Scientific, Inc.; REBS, Radiation and Energy Balance Systems, Inc.; SWFWMD, Southwest Florida Water Management District; negative height is depth below land surface.

<sup>a</sup> The use of firm, trade, and brand names in this report is for identification purposes only and does not constitute endorsement by the US Geological Survey.

environments. Generally, nighttime ET is negligible because of the low energy availability in the absence of solar radiation. Exceptions to this generalization can occur in open water or wetland environments where nighttime energy for  $ET_a$  can be derived from cooling of water. Nighttime  $ET_a$  was assumed to be zero in this study at a pasture site.

The canopy energy balance (Eqs. (1) and (2)) can serve as a valuable tool to further refine the evapotranspiration measurement

$$R_n - G = LE + H, \quad (1)$$

$$LE = \frac{R_n - G}{1 + B}, \quad (2)$$

where  $R_n$  is net radiation;  $G$  is soil heat flux at land surface;  $LE$  is the latent heat flux (the energy equivalent of  $ET_a$ );  $H$  is sensible heat flux;  $B$  is the Bowen ratio, equal to the ratio of sensible to latent heat flux; and the storage of heat in the canopy and

energy consumed by photosynthesis are assumed negligible.

Several investigators (Moore, 1976; Dugas et al., 1991; Goulden et al., 1998; Mahr, 1998; Twine et al., 2000; Brotzge and Crawford, 2003) noted that eddy correlation-measured fluxes of  $LE$  and  $H$  often are inconsistent with the energy balance for reasons discussed by Mahr (1998); generally the sum of the turbulent fluxes ( $LE + H$ ) is less than the measured available energy ( $R_n - G$ ). For example, Twine et al. (2000) noted that the period-of-record energy balance closure (defined as the ratio of the turbulent fluxes to the available energy) varied from 0.71 to 0.91 among several grassland sites. Twine et al. (2000) suggested that: (1) the error in the measured turbulent fluxes, and not error in measured available energy, was the primary source of energy-balance misclosure; (2) eddy correlation measurements of turbulent fluxes should be adjusted for energy-balance closure; and (3) the preferred method of energy-balance closure is to

maintain the Bowen ratio. In this ‘Bowen-ratio closure method’ suggested by Twine et al. (2000), the Bowen ratio is computed based on the measured values of  $H$  and  $LE$  and an energy balance-corrected value of  $LE$  is computed (Eq. (2)). German (2000) provided empirical support for the utility of the eddy correlation system to adequately measure the Bowen ratio; simultaneous measurement of the Bowen ratio by two independent methods were made at a sawgrass wetland site in Florida using: (1) temperature and vapor-pressure differentials (Bowen, 1926) measured with Radiation and Energy Balances, Inc. instrumentation and (2) eddy correlation instrumentation identical to that used in this study. Average latent heat flux (computed using the Bowen-ratio closure method) differed between the two methods by less than 1% over the three-month study period; this consistency is despite the energy-balance closure of 0.83 based on the turbulent fluxes uncorrected by the Bowen-ratio closure method. Further empirical support for the Bowen-ratio closure method was provided by a comparison of evapotranspiration estimated as a water-budget residual at a forested wetland in Florida with that measured using eddy correlation methods (Sumner, 2001); the Bowen-ratio closure method provided greater consistency (+4.7% discrepancy) with the water-budget-derived estimate of evapotranspiration than did the eddy correlation values uncorrected with the energy budget (−11.3% discrepancy). Reported values of evapotranspiration in this study incorporate Bowen-ratio closure corrections to eddy correlation measurements. Measurements for which the Bowen-ratio closure correction more than halved or doubled the uncorrected latent heat flux were considered missing.

The available energy input to the canopy (left-hand side of Eq. (1)) was estimated as the difference between the measured net radiation and the ground heat flux into the soil surface. Soil heat flux at the surface was based on measurements from two soil heat flux plates buried 8 cm deep, coupled with estimates of the transient energy storage change in the upper 8 cm of soil. This latter term was estimated based on measurements from eight thermocouples buried 2–6 cm deep and estimated soil heat capacity. The soil heat capacity was calculated from soil moisture measurements with a water content reflectometer placed in the upper 8 cm of soil and estimated

values of bulk density, specific heat of water, and specific heat of dry soil of  $1.35 \text{ g cm}^{-3}$ , 4190 and  $840 \text{ J kg}^{-1} \text{ }^\circ\text{C}^{-1}$ , respectively.

The source area of an eddy correlation measurement generally extends an upwind distance of about 100 times the sensor height (Stannard, 1993). With this criterion and a sensor height of 2.7 m, the source area to the west of the station includes the intended surface cover of pasture, as well as a residential area bordering the lake. Flux data obtained when wind direction was from an estimated  $80^\circ$  arc of inadequate fetch to the west (Fig. 1) were culled. A field to the east of the station was converted from pasture to strawberries/millet in September 2001, resulting in inadequate fetch within a  $65^\circ$  arc to the east. Flux data obtained following the field conversion and during winds from this eastern arc also were culled from the measured data. Application of an analytical solution of a one-dimensional (upwind) diffusion equation for a uniform surface cover (Schuepp et al., 1990), assuming mildly unstable conditions (Obukhov stability length of  $-10$  to  $-30 \text{ m}$ ) typical of daytime hours, indicated that 80–85% of the source area was contained within the radius given by 100 times sensor height. The adequacy of the 100:1 guideline for extent of the source area was evaluated based on a search for wind-directional bias in the residuals of measured  $ET_a$  and that simulated with an ET model (modified Priestley–Taylor) independent of wind direction.

Green-leaf area index (LAI) of grass near the eddy correlation station was estimated on a monthly basis by using visual inspection in the manner described by Stannard (1993) and detailed below. Sunlit leaf area per unit area ( $L_s$ ) is given by Monteith and Unsworth (1990, p. 74) as

$$L_s = \frac{(1 - e^{-K_s L})}{K_s}, \quad (3)$$

where  $K_s$  is the canopy extinction coefficient and  $L$  is the one-sided leaf area index. As shown by Monteith and Unsworth (1990, p. 75),  $K_s \sim 1$  for all ellipsoidal leaf angle distributions at a solar elevation of  $30^\circ$ . Therefore at a solar elevation of  $30^\circ$ , Eq. (3) can be simplified to:

$$L = -\ln(1 - L_s). \quad (4)$$

Leaf area visible in a photo at 30° below horizontal is the same as sunlit leaf area at a solar elevation of 30°. The visually evaluated areal fraction of green leaves near the center of a photo taken at 30° was used to estimate  $L_s$  in Eq. (4). LAI was estimated for any given time based on a function of day of year fitted to the values of LAI estimated by the visual inspection method (Fig. 3). A sine curve satisfactorily matched much of the annual trend in LAI. However, a typical late-March to early-June drought pattern (Fig. 2a) produced grass browning that was simulated with a linear trend over about a 2.5-month period. The low frequency of LAI measurements prevented precise definition of the regreening in June. Because observations indicate that regreening of grass in Florida occurs within several days, the regreening is approximated as coinciding with the beginning of the wet season on June 5, 2001. Fig. 3 shows the evolution of the LAI as a function of time for June 6 through March 22 as

$$L = a \sin(\omega(t - b)) + c, \quad (5a)$$

and for March 23 to June 5 as

$$L = dt + e, \quad (5b)$$

where  $\omega$  is angular velocity of the Earth about the Sun ( $2\pi/365$ ), in per day;  $t$  is day of year;  $a$  ( $=0.75$ ),  $b$  ( $=92$ ), and  $c$  ( $=0.78$ ) are regression-estimated parameters; and  $d$  ( $=-0.0055$ ) and  $e$  ( $=1.10$ ) are parameters based on the observed trend in LAI from March–May 2001. The LAI function (Eqs. (5a) and (5b)) reproduced measured LAI values with a coefficient of determination ( $r^2$ ) of 0.96.

### 3.2. Weather station

The long-term weather station is located about 400 m from the eddy correlation station in a patch of Bahia grass on the side of a dirt road, between a pasture and a strawberry/millet field (Fig. 1). This station is part of a larger network of weather stations in the Southwest Florida Water Management District. Data (hourly resolution) collected at network stations includes rainfall, air temperature, relative humidity, incoming solar radiation, wind speed, and wind direction (Table 1). A standard weather bureau Class A evaporation pan (122 cm diameter by 25 cm height) at the weather station was manually (hook gage) measured. The water level in the pan was maintained within 7.5–12.5 cm of the lip. The pan is

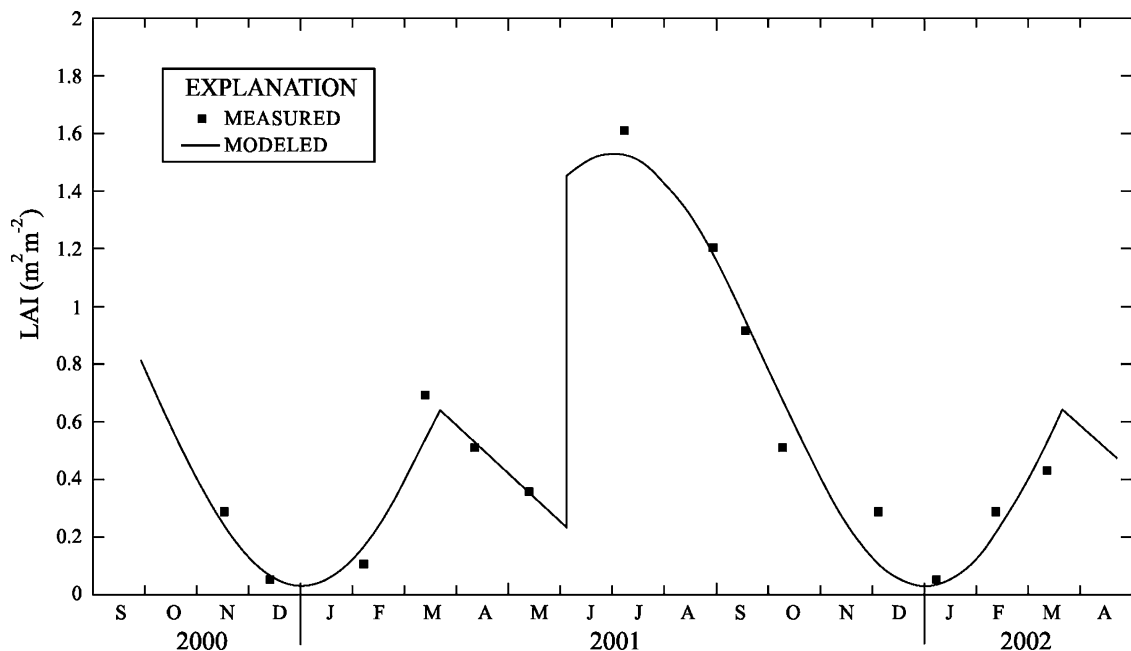


Fig. 3. Observations and modeled (Eq. (5)) values of pasture green-leaf area index (LAI).

noninsulated and rests on a wooden platform 13 cm above the ground. Nonirrigated grass grows to the edge of the wooden frame, although the dirt road and the planted field are within 6 and 10 m, respectively, of the evaporation pan. Daily  $E_p$  measurements were made at about 8:00 a.m. Generally, measured  $E_p$  must be corrected for any additions of rainfall to the pan. However, errors in rainfall measurement and inconsistency in rainfall capture between a rain gage and an evaporation pan can add error to measured  $E_p$ . Therefore, some  $E_p$  data were culled from the dataset by removing measurements representing 24-h periods when rain occurred. During the study period, many daily values of  $E_p$ , and occasionally entire months, were missing because measurements were not made or because of rainfall.

## 4. Theory and models

### 4.1. Penman–Monteith evapotranspiration (PM)

The PM equation is a generalization of the Penman equations that allows for a composited plant stomatal resistance to vapor transport that is specified through a bulk surface resistance (Penman, 1948; Monteith, 1965). The PM equation typically is written in terms of LE

$$LE = \frac{\Delta(R_n - G) + \rho_a c_p (e_s - e)/r_a}{\Delta + \gamma(1 + r_s/r_a)}, \quad (6)$$

where  $\Delta$  is slope of the saturation vapor-pressure curve;  $\rho_a$  is mean air density at constant pressure;  $c_p$  is specific heat of air;  $e_s - e$  is the vapor-pressure deficit;  $e_s$  is saturation vapor-pressure of the air;  $e$  is actual vapor-pressure of the air;  $\gamma$  is the psychrometric constant;  $r_s$  is bulk surface resistance;  $r_a$  is aerodynamic resistance; and other variables are as previously defined.

The aerodynamic resistance was estimated using Monin–Obukhov similarity and assuming neutral conditions by

$$r_a = \frac{\ln[(z - d)/z_o] \ln[(z - d)/z_{ov}]}{k^2 u}, \quad (7)$$

where  $z$  is height at which wind speed is measured;  $d$  is displacement height;  $z_o$  is roughness height for

momentum;  $z_{ov}$  is roughness height for water vapor;  $k$  is von Karman's constant, equal to 0.4; and  $u$  is horizontal wind speed at sensor height  $z$ .

The variable  $d$  may be estimated as equal to  $0.67z_{veg}$  (Brutsaert, 1982), where  $z_{veg}$  is the vegetation height;  $z_o$  may be approximated as  $0.1z_{veg}$  (Dingman, 1994); and  $z_{ov}$  may be approximated as  $0.1z_o$  (Jensen et al., 1990). The assumption of neutral stability in Eq. (7) is usually not met at the site; daytime conditions generally are unstable. Stability corrections require data not readily available from typical weather stations (i.e. sensible and latent heat fluxes; Paulson (1970)) and, therefore, the utility of a PM equation uncorrected for stability was evaluated in this study.

### 4.2. Penman–Monteith reference evapotranspiration ( $ET_0$ )

$ET_0$  is 'the rate at which water, if available, would be removed from the soil and plant surface of a specific crop, arbitrarily called a reference crop' (Jensen et al., 1990). In this study,  $ET_0$  is defined by the American Society of Civil Engineers (ASCE) (Walter et al., 2000) and the Food and Agricultural Organization (FAO) (Allen et al., 1998) standard, hypothetical 12-cm grass reference crop under well-watered conditions, a fixed surface resistance of  $70 \text{ s m}^{-1}$  (Jensen et al., 1990), and an albedo of 0.23. Application of reference conditions in Eq. (6) yields

$$ET_0 = \frac{0.408\Delta(R_n - G) + \gamma \frac{C_n}{T+273} u_2 (e_s - e)}{\Delta + \gamma(1 + C_d u_2)}, \quad (8)$$

where  $ET_0$  is the standardized reference crop ET ( $\text{mm day}^{-1}$  for daily time steps or  $\text{mm h}^{-1}$  for hourly time steps);  $R_n$  is net radiation at the crop surface ( $\text{MJ m}^{-2} \text{ day}^{-1}$  for daily time steps or  $\text{MJ m}^{-2} \text{ h}^{-1}$  for hourly time steps);  $G$  is soil heat flux at the soil surface ( $\text{MJ m}^{-2} \text{ day}^{-1}$  for daily time steps or  $\text{MJ m}^{-2} \text{ h}^{-1}$  for hourly time steps);  $T$  is mean daily or hourly air temperature at 1.5–2.5-m height ( $^{\circ}\text{C}$ );  $u_2$  is mean daily or hourly wind speed at 2-m height ( $\text{m s}^{-1}$ );  $e_s$  is mean saturation vapor-pressure at 1.5–2.5-m height (kPa) (for daily computation, the value is the average of  $e_s$  at maximum and minimum air temperature);  $e$  is mean actual vapor-pressure at

1.5–2.5-m height (kPa);  $\Delta$  is slope of the saturation vapor-pressure-temperature curve (kPa °C<sup>-1</sup>);  $\gamma$  is psychrometric constant (kPa °C<sup>-1</sup>);  $C_n$  is numerator constant for reference type and calculation time step; and  $C_d$  is denominator constant for reference type and calculation time step. For daily time steps, the constants  $C_n$  and  $C_d$  are 900 and 0.34, respectively. The values of  $R_n$  and  $G$  in Eq. (8) are estimated from measured values of incoming solar radiation as described by Walter et al. (2000).

#### 4.3. Priestley–Taylor evapotranspiration (PT)

The Priestley–Taylor approach for estimating evaporation from an extensive wet surface under conditions of minimum advection (Priestley, 1959; Slatyer and McIlroy, 1961; Priestley and Taylor, 1972) is described as

$$LE = \alpha \frac{\Delta}{\Delta + \gamma} (R_n - G), \quad (9)$$

where  $\alpha = 1.26$  is an empirically determined dimensionless correction. Eq. (9), valid for conditions of potential  $ET_a$  is a simplification of the PM equation.

The modified Priestley–Taylor approach (Flint and Childs, 1991) is a generalization of the original Priestley–Taylor approach to allow for nonpotential conditions:

$$LE = \alpha(\text{environment}) \frac{\Delta(R_n - G)}{\Delta + \gamma}. \quad (10)$$

In the modified approach,  $\alpha$  is a function of environmental variables. A unique, physics-based functional form for the modified Priestley–Taylor  $\alpha$  has not been defined and must be determined empirically.

## 5. Results

About 45% of the daytime values of 30-min  $ET_a$  were measured and the remainder were deemed missing. Missing measurements were the result of culled data under conditions of: wind direction with inadequate fetch (55% of missing values), obscured hygrometer windows (21%), excessive misalignment of sonic anemometer (<1%), and/or excessive

energy-budget correction (30%). Vapor flux corrections for density fluctuations and hygrometer sensitivity to oxygen averaged 5 and 2%, respectively. Energy-balance closure averaged 74%, within the range of grassland closure values noted by Twine et al. (2000).

#### 5.1. Penman–Monteith (PM) model for 30-min $ET_a$

Bulk surface resistance was estimated by applying meteorological data and eddy correlation measurements of LE to the inverted PM (Eq. (6)). The bulk surface resistance was considered as a function of several environmental variables: air temperature, wind speed, vapor-pressure deficit, LAI, net radiation, and soil moisture in the upper 30 cm using linear and nonlinear relationships. Net radiation and vapor-pressure deficits were identified as explanatory variables. Martin et al.'s (1997) approach was used to develop an empirical model between the bulk surface conductance  $g_s (= 1/r_s)$  and the net radiation and vapor-pressure deficit  $D$  such that

$$g_s = f(D)g_{\max}(R_n), \quad (11)$$

where  $g_{\max}(R_n)$  relates the maximum conductance to  $R_n$  when  $D$  is not limiting  $g_s$ . The vapor-pressure function  $f(D)$ , reduces  $g_{\max}(R_n)$  based on the vapor-pressure deficit and ranges between 0 and 1. To model normal atmospheric conditions, abnormally high values of  $g_s$  ( $>0.015 \text{ m s}^{-1}$ ) comprising 7.5% of the data set were eliminated from the modeling data. A typical relation between  $g_s$  and  $D$  was observed with  $g_s$  ranging between about 0.001 and 0.015  $\text{m s}^{-1}$  ( $r_s$  between 67 and 1000  $\text{s m}^{-1}$ ) for  $D$  less than 0.7 kPa and  $g_s$  consistently below 0.006  $\text{m s}^{-1}$  for  $D$  greater than 3 kPa (Fig. 4a). The modeled  $g_s$  was bounded by the vapor-pressure deficit observations such that  $f(D) = -0.166 \ln(D) + 0.235$  and scaled using a linear relation between measured  $g_{\max}$  ( $g_{\max} = g_s/f(D)$ ) and  $R_n$  values determined to be  $g_{\max}(R_n) = 5.39 \times 10^{-5} R_n + 0.0033$  (Fig. 4b). Modeled values using the PM equation and the modeled  $g_s$  values agreed well with the measured values (Fig. 5). The 5159 30-min modeled ET values reproduced measured values with a standard error (SE) of 1.48  $\text{mm day}^{-1}$ , an  $r^2$  of 0.81, and negligible temporal variations in error bias. The SE for daily

composites of 30-min PM ET estimates can be approximated as  $0.15 \text{ mm day}^{-1}$  (the average of the SE of composited daytime values and an assumed nighttime SE of zero). The SE of composited daytime values was approximated as the SE of 30-min values divided by the square root of 24 (average number of daytime values in a day).

### 5.2. Priestley–Taylor (PT) model for 30-min $ET_a$

In this study, as in previous studies (Sumner, 1996; German, 2000), a range of parameterized models for PT  $\alpha$  composed of simple combinations of environmental variables were evaluated in a trial-and-error fashion. These environmental variables included: air

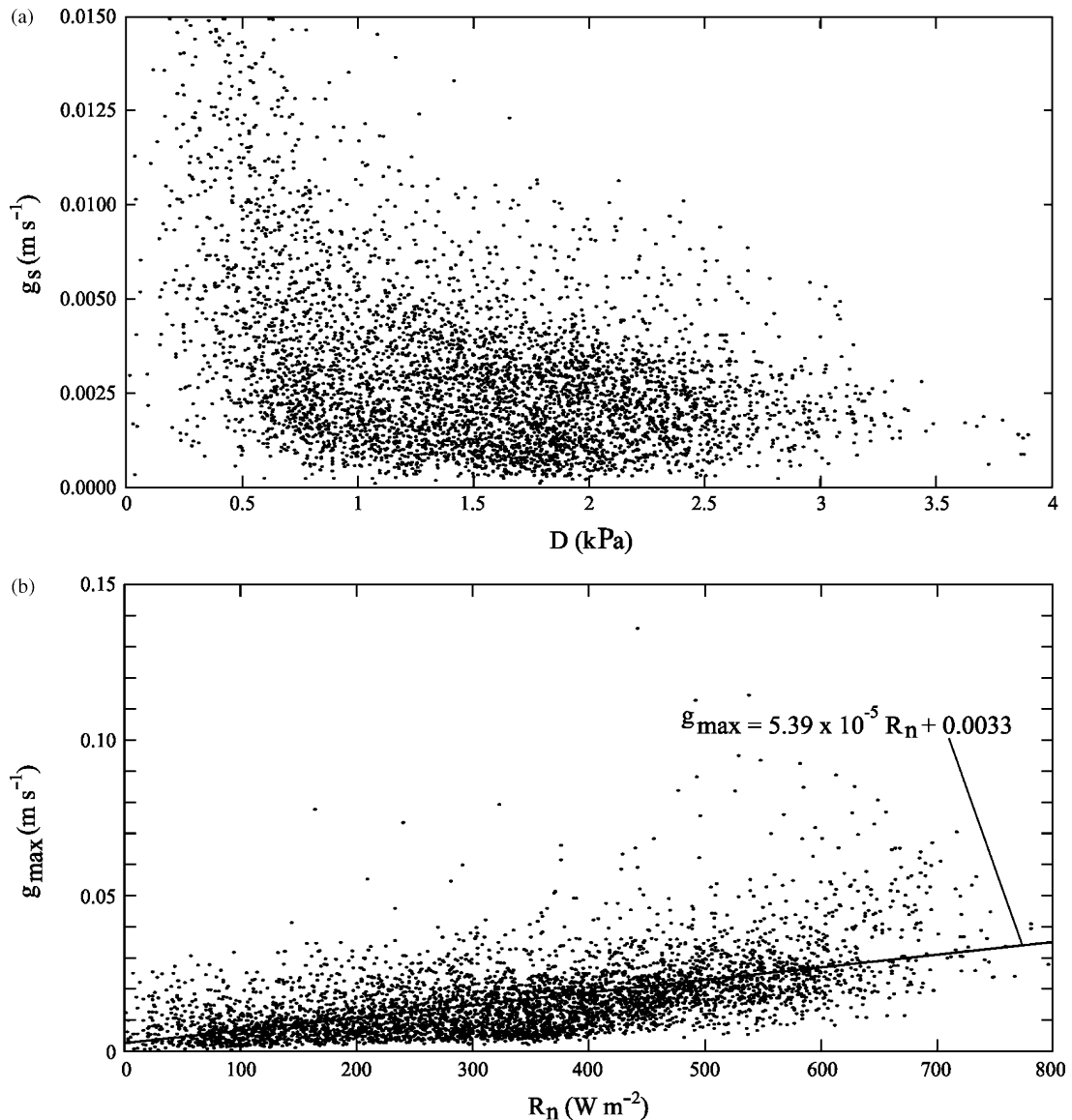


Fig. 4. (a) Bulk surface conductance ( $g_s$ ) relative to vapor-pressure deficit ( $D$ ); (b) maximum bulk surface conductance ( $g_{\max}$ ) relative to net radiation ( $R_n$ ).

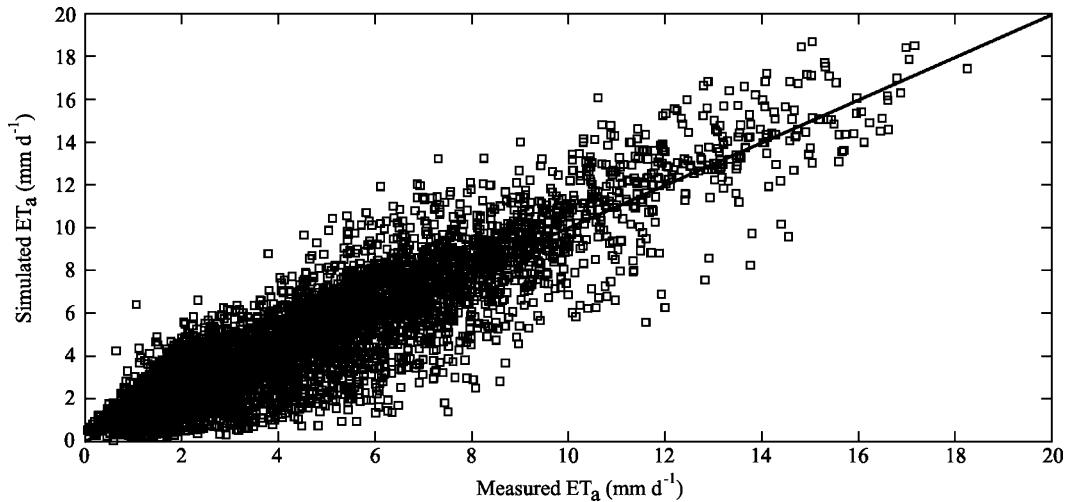


Fig. 5. Measured, 30-min resolution evapotranspiration rate and evapotranspiration rate modeled by the Penman–Monteith equation (Eq. (6)) with the bulk surface conductance estimated by Eq. (11). The 1:1 line is also shown.

temperature, wind speed, vapor-pressure deficit, LAI, incoming solar radiation, and soil moisture in the upper 30 cm. Parameters within  $\alpha$  were estimated by using regression between measured and simulated values of  $ET_a$ . The relative significance of individual variables in the evaluated models was determined based on the normalized SE for the parameter associated with a given variable in the model. Incoming solar radiation and LAI were relatively significant explanatory variables for the  $\alpha$  function; other tested variables contributed relatively little explanatory value and were excluded for simplicity. The final form of the modified PT  $\alpha$  function is described by

$$\alpha = (aS + bS^2 + c)(dL + 1), \quad (12)$$

where  $S$  is incoming solar radiation ( $W\ m^{-2}$ );  $L$  is one-sided LAI ( $m^2\ m^{-2}$ ); and  $a$  ( $= -9.95 \times 10^{-4}$ ),  $b$  ( $= 6.36 \times 10^{-7}$ ),  $c$  ( $= 0.801$ ), and  $d$  ( $= 0.657$ ) are the best fit parameters estimated from the regression relation of the PT-estimated values of  $ET_a$  against measured values of  $ET_a$ .

The PT  $\alpha$  function (Eq. (12)) reproduced 5159 measured values of 30-min resolution ET (Fig. 6) with a SE of  $1.08\ mm\ day^{-1}$ , an  $r^2$  of 0.88, and negligible temporal variations in error bias. The SE for daily composites of 30-min PT ET estimates can be approximated as  $0.11\ mm\ day^{-1}$ . As modeled by

Eq. (12),  $\alpha$  increased linearly with LAI and varied by about a factor of two, for a given value of solar radiation, over the range of LAI values present during the experiment (Fig. 7).

Within the modified Priestley–Taylor approach (Eq. (10)), partitioning of available energy ( $R_n - G$ ) into latent and sensible heat fluxes is governed by the environmental variables within the PT  $\alpha$  function (Eq. (12)) and air temperature (through the dependence of  $\Delta/(\Delta + \gamma)$  on air temperature). Given the depth of the water table below the rooting zone (probably more than 4 m) and the low capillarity of sandy soils, soil moisture fluctuations might be expected to affect  $ET_a$ . However, the measured shallow soil moisture (upper 30 cm) was not a significant explanatory variable for  $ET_a$ . The measured shallow soil moisture does not fully represent the soil moisture status within the deep rooting zone of Bahia grass. However, much of the explanatory power of rooting-zone soil moisture is contained within LAI, because grass growth is stimulated by rooting-zone soil moisture; explicit differentiation of the effect of soil moisture and LAI on  $ET_a$  may be difficult.

A comparison of the residuals between the calibrated modified Priestley–Taylor model and measured values of  $ET_a$  showed negligible wind-directional bias, despite the much greater fetch of pasture along the north–south axis. This observation

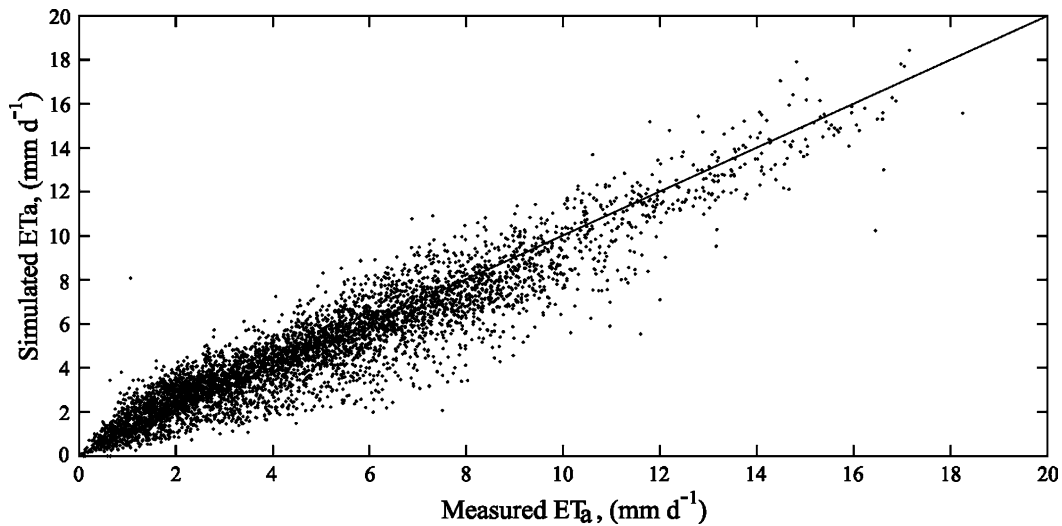


Fig. 6. Measured, 30-min resolution evapotranspiration rate and evapotranspiration rate modeled by the modified Priestley–Taylor equation (Eq. (10)) with the Priestley–Taylor  $\alpha$  estimated by Eq. (12). The 1:1 line is also shown.

supports the assumption that the measured values of  $ET_a$  were representative of the pasture.

### 5.3. Evapotranspiration and energy fluxes

Daily values of  $ET_a$  were derived from measured 30-min data, along with gap-filling with the site-calibrated, PT model (Eqs. (10) and (12)). Of the total  $ET_a$  of 1079 mm during the study period, 512 and 567 mm were measured and gap-filled, respectively. Because  $E_p$  measurements were made at 8:00 a.m., daily values of  $E_p$  represent an 8:00-to-8:00 a.m. 24-h period. Daily values of  $ET_0$  and  $ET_a$  were compiled for a similar time interval for consistency of comparison. Daily values of  $ET_a$  ranged from less than 1 mm in early winter to more than 4 mm on clear summer days (Fig. 8). The relatively high day-to-day variability in  $ET_a$  reflects the high variability in cloud cover observed during the summer. Total  $ET_a$  was 773, 787, and 789 mm for the 1-year periods beginning September 29, 2000, January 1, 2001, and April 24, 2001, respectively.

The evolution of the turbulent fluxes of latent and sensible heat during the study period are shown in Fig. 9 and Table 2. Soil heat flux generally was a small component of the daily canopy energy budget. The Bowen ratio for the study period clearly shows that

the partitioning of available energy into latent and sensible heat flux exhibits seasonal changes (Fig. 10 and Table 2). The results indicate that increases in green-leaf density increase that portion of available energy used for  $ET_a$ . These observations reinforce the importance of characterizing seasonal and drought-induced transitions in pastures from living green leaves that transpire water to senescent brown leaves that do not. The effect of air temperature on partitioning of available energy may be considered based on the Priestley–Taylor equation (Eq. (9)) where the multiplier  $\Delta/(\Delta + \gamma)$  varies from about 0.4 at 0 °C to 0.78–30 °C. In the June–August 2001 growing season, when LAI and air temperature reached peak values, about 68% of the available energy was directed to latent heat flux. Only 47% of the available energy was directed to latent heat flux during the remainder of 2001.

### 5.4. Comparison of actual evapotranspiration ( $ET_a$ ) and pan evaporation ( $E_0$ )

$ET_0$  was computed based on data collected at the weather station and the FAO 1998 Penman–Monteith approach (Eq. 8). The relations between  $ET_a$  and  $ET_0$  are shown in Fig. 8 and Table 3. Daily values of  $ET_0$  exceeded  $ET_a$  on average by about 42% for 2001. The relative difference varied seasonally.

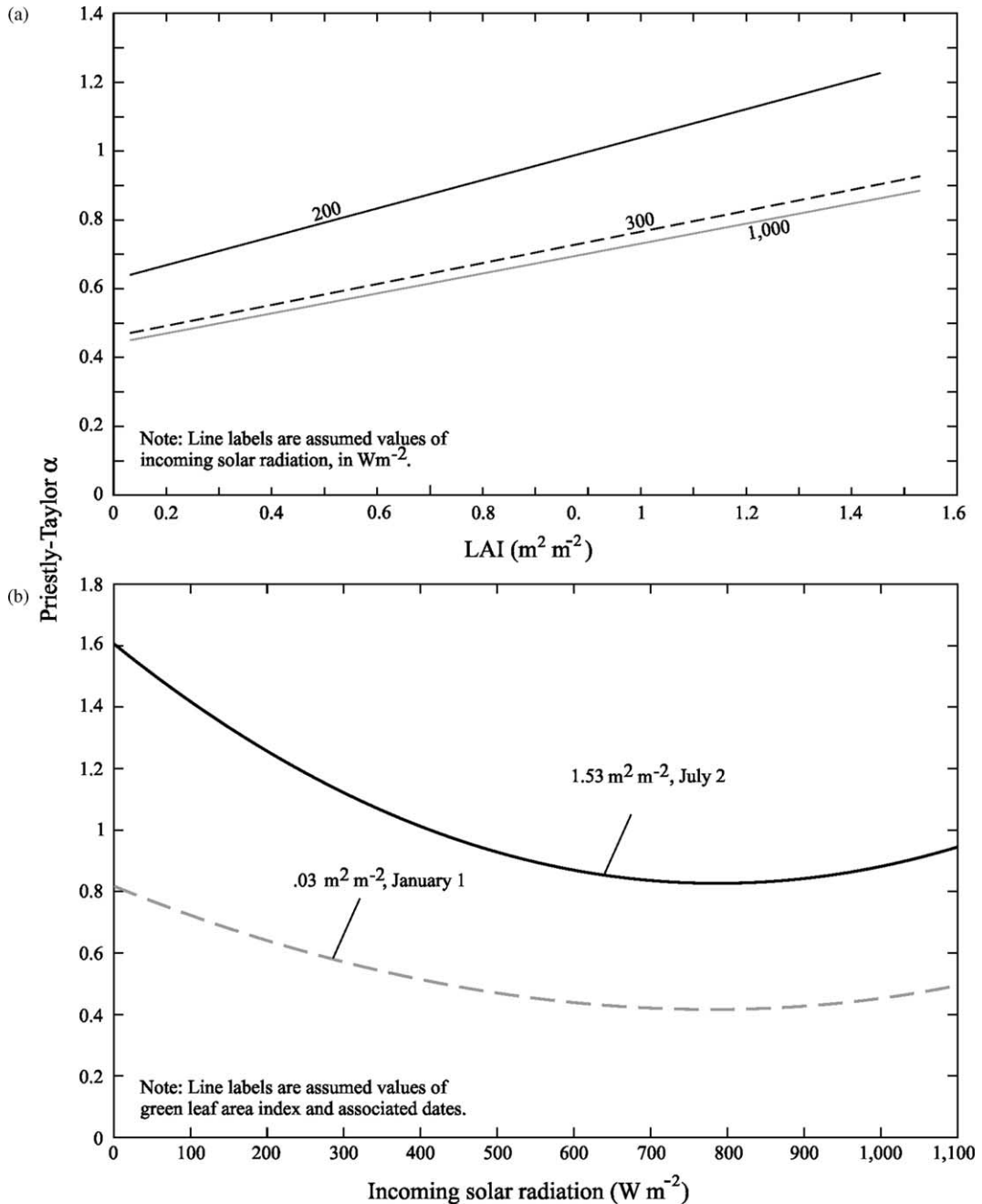


Fig. 7. Modeled values of the Priestley–Taylor  $\alpha$  estimated by Eq. (12) as a function of (a) green leaf area index and (b) incoming solar radiation.

The smallest relative difference between  $\text{ET}_a$  and  $\text{ET}_0$  occurred during the wet season when the density of green grass most closely approximated the condition assumed by the  $\text{ET}_0$  method.

The vegetation coefficient, determined from the ratio of  $\text{ET}_a$  to  $\text{ET}_0$ , showed substantial variability throughout the study period (Fig. 11). The abrupt increase in the vegetation coefficient on June 6, 2001,

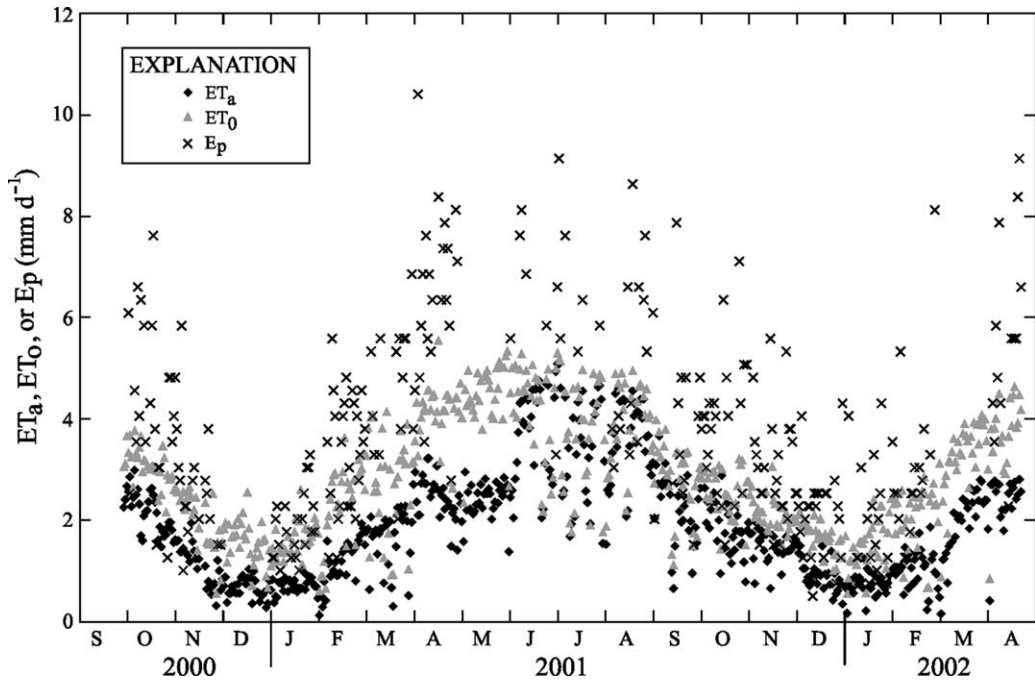


Fig. 8. Daily values of actual evapotranspiration ( $ET_a$ ), reference evapotranspiration ( $ET_0$ ), as computed by Eq. (8), and pan evaporation ( $E_p$ ).

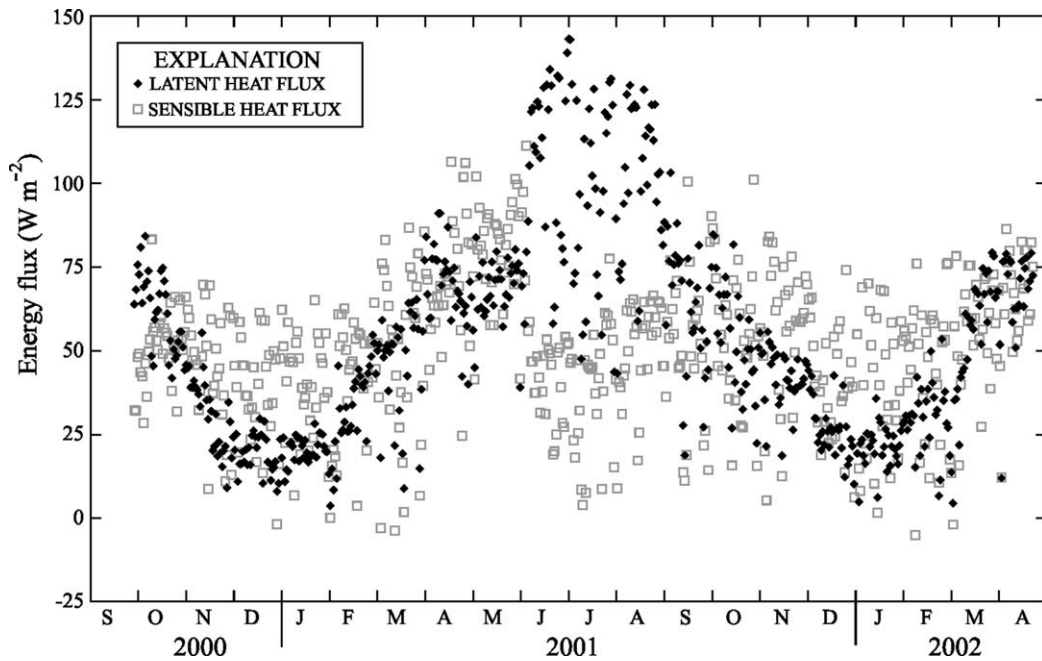


Fig. 9. Daily average values of turbulent fluxes of latent heat and sensible heat.

Table 2  
Average monthly values of energy fluxes and ratios

Month	Incoming solar radiation	Net radiation	Soil heat flux	Latent heat flux	Sensible heat flux	Bowen ratio	Evaporative fraction
Oct-00	215	110	-3	60	52	0.87	0.53
Nov-00	157	70	-7	31	46	1.47	0.40
Dec-00	140	50	-8	19	39	2.05	0.33
Jan-01	150	56	-3	20	39	1.95	0.34
Feb-01	164	78	1	34	43	1.28	0.44
Mar-01	187	91	-3	47	48	1.03	0.49
Apr-01	276	143	2	70	71	1.01	0.50
May-01	288	154	4	69	81	1.17	0.46
Jun-01	252	150	1	100	48	0.48	0.68
Jul-01	226	142	2	100	40	0.40	0.71
Aug-01	236	153	2	101	51	0.50	0.67
Sep-01	180	111	-3	64	50	0.79	0.56
Oct-01	178	108	-3	55	56	1.02	0.49
Nov-01	152	96	-3	42	57	1.36	0.42
Dec-01	130	64	-5	27	41	1.52	0.40
Jan-02	129	59	-3	22	40	1.86	0.35
Feb-02	169	70	-8	31	46	1.49	0.40
Mar-02	216	107	0	54	53	0.98	0.50

All energy fluxes are in watts per square meter; Bowen ratio and evaporative fraction are dimensionless.

corresponded to a rapid increase in LAI in response to the onset of the summer wet season. A regression analysis was conducted to relate  $ET_a$  to  $ET_0$  using physical variables. Air temperature, wind speed, vapor-pressure deficit, LAI, incoming solar radiation, and soil moisture were considered as explanatory variables for this relation; LAI demonstrated the most

explanatory value. The equation relating  $ET_a$  to  $ET_0$  is

$$ET_a = (aL + b)ET_0, \quad (13)$$

where  $ET_a$  and  $ET_0$  are in  $\text{mm day}^{-1}$ ;  $L$  is LAI as a function of time, in  $\text{m}^2 \text{m}^{-2}$ ; and  $a$  ( $=0.330$ ) and  $b$  ( $=0.451$ ) are parameters estimated through regression of daily values of  $ET_0$  against measured

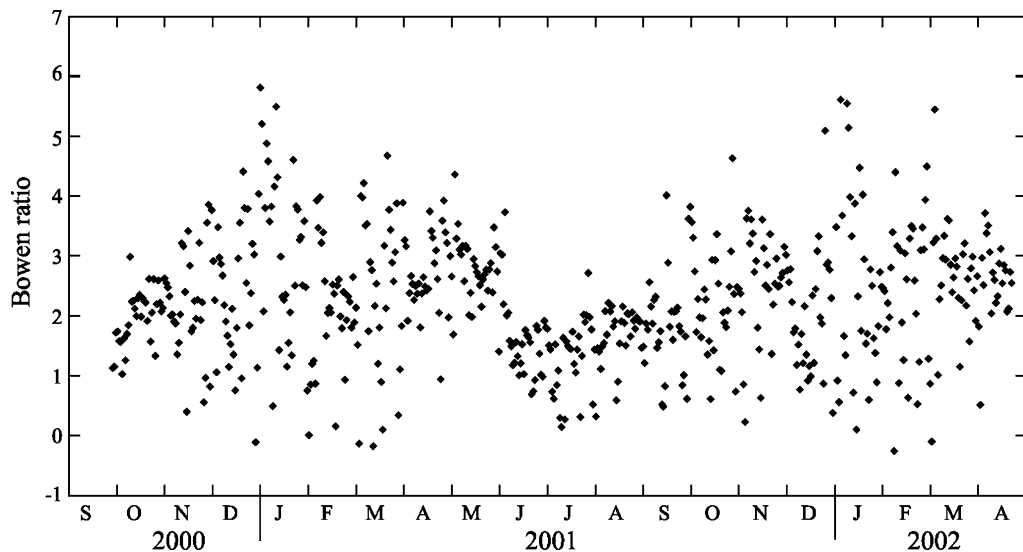


Fig. 10. Daily values of the Bowen ratio.

Table 3

Monthly rainfall, actual evapotranspiration, reference evapotranspiration, and pan evaporation; and monthly vegetation and pan coefficients

Month	No missing data				Some missing pan evaporation data				
	Rainfall	Actual evapotranspiration	Reference evapotranspiration	Vegetation coefficient	Number of days of measured pan evaporation	Actual evapotranspiration <sup>a</sup>	Pan evaporation <sup>a</sup>	Reference evapotranspiration <sup>a</sup>	Pan coefficient
Oct-00	3	2.13	3.05	0.70	22	2.23	4.33	3.12	0.51
Nov-00	35	1.10	2.00	0.55	18	1.24	2.77	2.11	0.45
Dec-00	30	0.67	1.57	0.42	0	–	–	–	–
Jan-01	69	0.70	1.59	0.44	22	0.73	1.91	1.59	0.39
Feb-01	6	1.19	2.38	0.50	24	1.30	3.37	2.62	0.39
Mar-01	197	1.64	2.78	0.59	14	1.94	4.64	3.10	0.42
Apr-01	0	2.47	4.08	0.61	22	2.48	6.33	4.15	0.39
May-01	37	2.44	4.53	0.54	0	–	–	–	–
Jun-01	231	3.57	4.18	0.85	5	4.05	6.81	4.91	0.60
Jul-01	223	3.55	3.85	0.92	8	4.72	6.22	4.97	0.76
Aug-01	75	3.59	3.96	0.91	13	3.83	5.16	4.23	0.74
Sep-01	299	2.27	2.81	0.81	11	2.29	4.02	2.97	0.57
Oct-01	13	1.94	2.59	0.75	23	2.03	3.89	2.67	0.52
Nov-01	5	1.49	2.14	0.69	23	1.46	3.05	2.09	0.48
Dec-01	9	0.96	1.69	0.57	24	0.96	2.19	1.70	0.44
Jan-02	81	0.76	1.56	0.49	18	0.80	2.06	1.65	0.39
Feb-02	77	1.09	2.08	0.52	17	1.20	2.93	2.23	0.41
Mar-02	53	1.90	3.24	0.59	0	–	–	–	–

Units in millimeters per day, with exception of vegetation coefficient and pan coefficients (dimensionless) and rainfall (mm). Vegetation coefficient is defined as actual evapotranspiration divided by reference evapotranspiration. Pan coefficient is defined as actual evapotranspiration divided by pan evaporation.

<sup>a</sup> Values refer to the average measured rate during the days of the given month with measured pan evaporation.

values of ET. The simulated vegetation coefficient ( $k_c$ ) is then given by:

$$k_c = aL + b. \quad (14)$$

Here, the vegetation coefficient increases linearly with increasing LAI. Eq. (13) reproduced the 570 measured values of daily resolution  $ET_a$  with a SE of  $0.29 \text{ mm day}^{-1}$ , an  $r^2$  of 0.93, and negligible temporal variations in error bias (Fig. 12).

### 5.5. Comparison of daily $ET_a$ and $E_p$

Only 277 measured values of  $E_p$  were available for comparison with  $ET_a$  because of missing or rain-culled data. Daily values of  $E_p$  generally exceeded  $ET_a$  (Fig. 8 and Table 3), by an average of more than 100% on an annual basis. The pan coefficient (defined as ratio of  $ET_a$  to  $E_p$  in this study) showed

considerable variability and no obvious systematic pattern (Fig. 13).

Regression analysis was used to relate  $ET_a$  to  $E_p$ . Application of a constant pan coefficient produced a very poor relation ( $r^2=0.38$ ). As with the actual-to-reference relation, a variety of environmental variables were considered as explanatory variables; again, LAI demonstrated the most explanatory value. The equation relating  $ET_a$  to  $ET_p$  is

$$ET_a = L(a + bE_p) + c, \quad (15)$$

where  $ET_a$  and  $E_p$  are in  $\text{mm day}^{-1}$ ; and  $a$  ( $=1.81$ ),  $b$  ( $=0.11$ ), and  $c$  ( $=0.782$ ) are parameters estimated through regression of daily values of  $E_p$  against measured values of  $ET_a$ . This equation reproduced 277 measured values of daily resolution ET with a SE of  $0.40 \text{ mm day}^{-1}$ , an  $r^2$  of 0.85, and negligible temporal variations in error bias (Fig. 14). The SE was about 19% of the average  $ET_a$ .

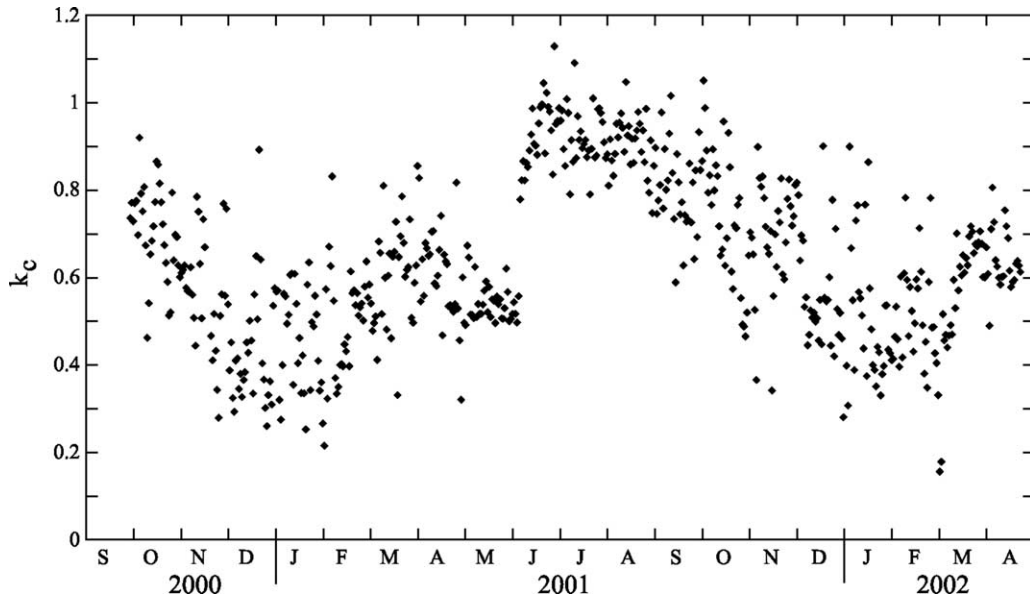


Fig. 11. Daily values of measured vegetation coefficient ( $k_c$ ).

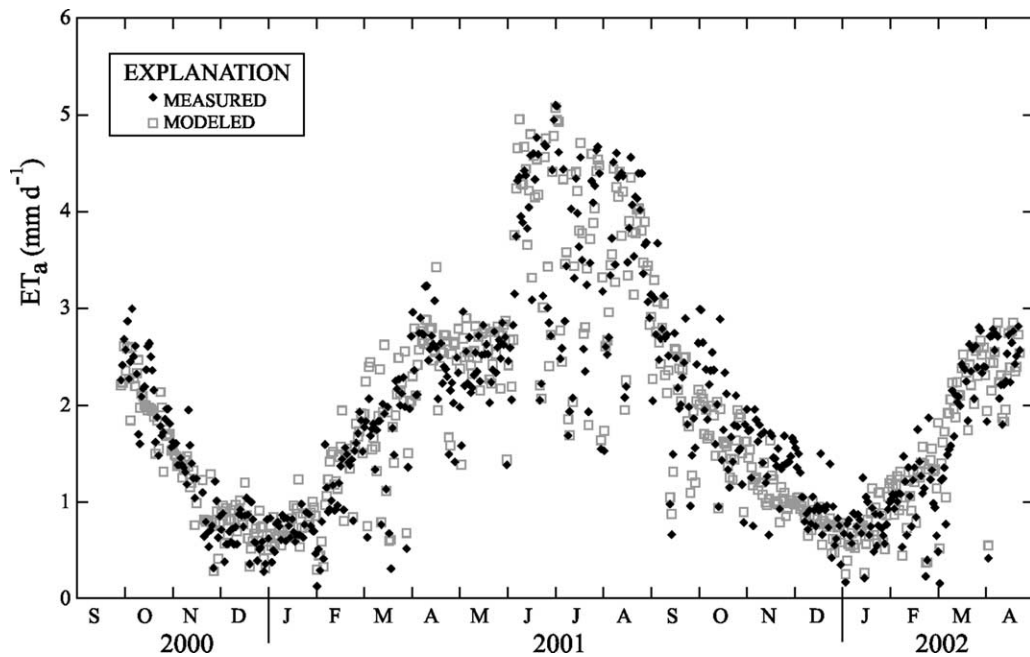


Fig. 12. Measured actual evapotranspiration and modeled actual evapotranspiration computed using reference evapotranspiration (Eq. (8)) with the vegetation coefficient estimated by Eq. (14).

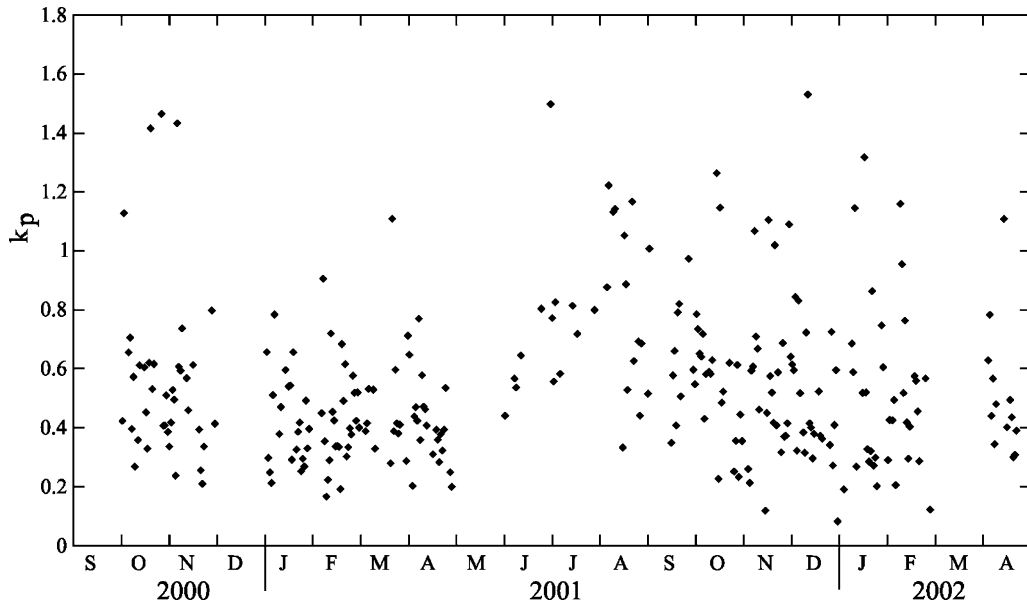


Fig. 13. Daily values of measured pan coefficients ( $k_p$ ).

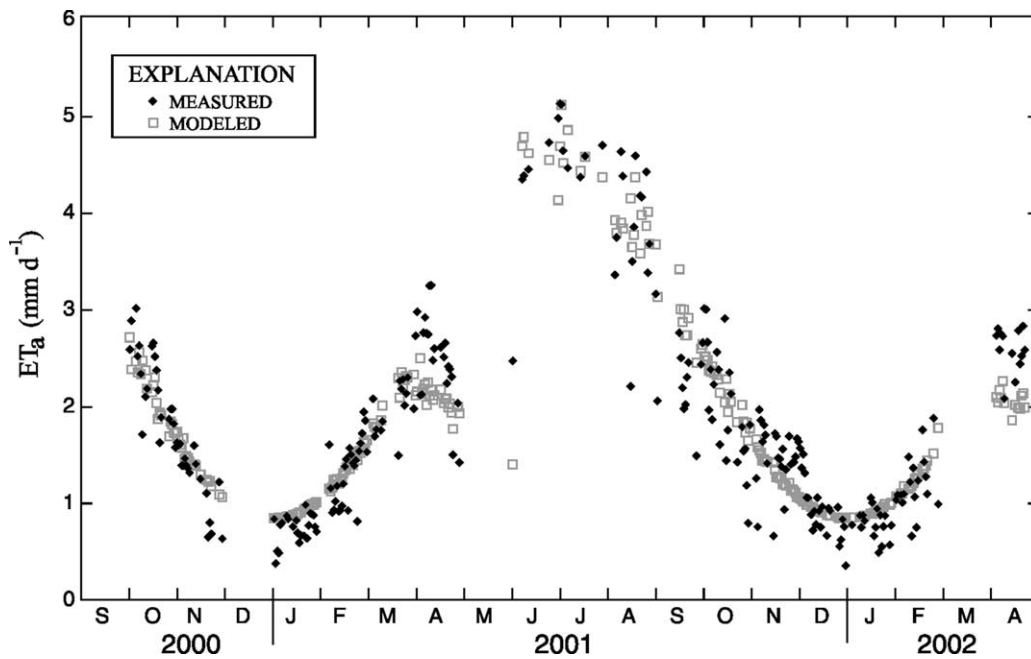


Fig. 14. Measured actual evapotranspiration and modeled actual evapotranspiration computed using measured pan evaporation with the pan coefficient estimated by Eq. (16).

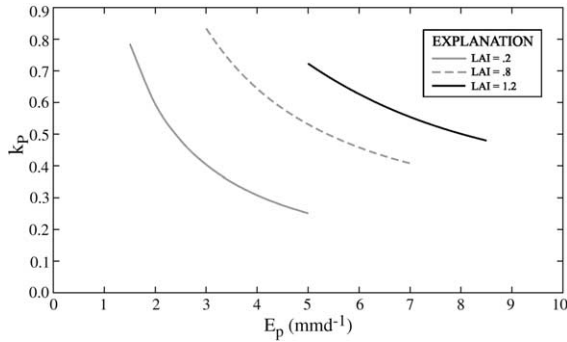


Fig. 15. Modeled values of the pan coefficient ( $k_p$ ) estimated by Eq. (16) as a function of pan evaporation ( $E_p$ ) and green leaf area index (LAI).

The simulated pan coefficient ( $k_p$ ) is given by:

$$k_p = \frac{(aL + c)}{E_p} + bL \quad (16)$$

In contrast to the  $ET_a$ -to- $ET_0$  relation (Eq. (14)), inclusion of a nonzero intercept was critical to an improved model relating  $E_p$  to  $ET_a$ . The implication of this difference is that the pan coefficient is a function not only of LAI, but also of  $E_p$  itself. Results indicate that the pan coefficient increases with increasing LAI and decreases with increasing  $E_p$  (Fig. 15). Linacre (2002) noted that pan coefficients generally decrease with increasing  $E_p$  as a result of disproportionally enhanced radiative and convective transfer of energy from the surrounding areas to the pan during periods of high  $E_p$ . Linacre (1994) presented a discussion of the heat budget for an evaporation pan. Solar radiation heats the evaporation pan through direct and diffuse radiation on the pan walls and through short-wave radiation reflected from the ground to the pan walls. If evaporative cooling of the area surrounding the pan is limited by soil moisture or green-leaf density, a temperature differential will develop between the surroundings and the pan, resulting in a net input of long-wave radiation to the pan from the surroundings. Additionally, convected heat (sensible heat) from the surroundings can provide further energy input to the evaporation pan, particularly in cases where partitioning of available energy to sensible heat is relatively high in the surroundings because of limiting values of soil moisture or green-leaf density. This phenomenon is an

example of the ‘oasis’ or ‘clothes-line’ effect. Dale and Scheeringa (1977) also noted the effect of dryness in the area around evaporation pans in increasing  $E_p$ .

## 6. Discussion

The relations of PT,  $ET_0$ , and  $E_p$  to  $ET_a$  depend on pasture LAI. Although LAI is not routinely measured at most weather stations, it could readily be incorporated through analysis of photographs taken during routine station maintenance. Remote sensing may also be used to quantify temporal changes in LAI. The normalized difference vegetation index (NDVI), a quantity that has been shown to be correlated to LAI (Asrar et al., 1989; Nemani and Running, 1989), is routinely computed from satellite-measured reflectances (Eidenshink, 1992). For example, from 1989 to 2004, the US Geological Survey Earth Resources Observation Systems Data Center has developed 1.1-km, weekly- and biweekly-composited NDVI products for the conterminous United States based on data from the Advanced Very High Resolution Radiometer aboard the NOAA polar-orbiting satellite series. At sites, such as the pasture site of this study, that are small relative to the 1.1-km NDVI resolution, NDVI could be estimated from a larger, but nearby and environmentally similar, pasture. A remote sensing approach has the advantage of being automated and less subjective than the visual analysis of photographs used in this study. Wang et al. (2003) noted that precipitation and temperature were strong indicators of NDVI (and therefore LAI) in the central Great Plains, USA, suggesting that the long-term record of these meteorological variables can serve to estimate LAI for the last several decades. Although the  $ET_0$  method of estimating  $ET_a$  was less effective than either the PM or PT methods, the reliance of this method on incoming solar radiation data, rather than net radiation and soil heat flux data as required by the PM and PT methods, is a distinct advantage of the  $ET_0$  method because of the relative abundance of solar radiation data.

A fundamental question concerns the transferability of the relations between PM, PT,  $ET_0$ , and  $E_p$  to  $ET_a$  at other sites and at other time periods. It is clear that these relations would be most appropriate for estimation of  $ET_a$  from an environmental setting

(Bahia grass pasture, humid, sandy soils, deep water table) similar to that from which these relations were obtained. Confidence in each of the relations was enhanced by their ability to estimate  $ET_a$  with negligible temporal bias in error. While, it must be acknowledged that the relations developed showed conclusive utility only *for the study site during the study period*, judicious use of current research's results combined with early studies may serve to reduce the conjecture involved in applying relations at other pasture sites or at the study site during other time periods. For example, the support of the PM equation with appropriate functional relationships concurs with Stewart and Gay's (1989) and Martin et al.'s (1997) results which indicate canopy conductance requires functional relationships based on vapor-pressure deficit and net radiation with site specific constants. In addition, the use of the PM- and PT-to- $ET_a$  relations at other sites requires that the measured meteorological variables be representative of a pasture. This objective will be difficult to meet at weather stations not placed in pastures, particularly in the measurement of net radiation, soil heat flux, and wind speed, all of which are relatively sensitive to the specific surface cover. Despite these qualifications, the relations developed in this study may represent the 'best available' method to meet the evapotranspiration data requirements for water management under the constraints of the sometimes prohibitively high costs of direct measurements of  $ET_a$  and the general rarity of historical measurements of  $ET_a$ . Further confidence in the relations could be developed with more direct measurements of  $ET_a$  at other sites and/or during other time periods.

The nonuniform siting of weather stations and evaporation pans limits transferability of the  $ET_0$ - and  $E_p$ -to- $ET_a$  relations to other sites. In this study, the weather station was not in an ideal site for computation of  $ET_0$ . The reference assumptions of a well-watered, fully green grass cover of uniform 8–12 cm height are most closely approached at this site in the wet season during noneastward winds (Fig. 1), but are violated at other times. However, nonideal conditions due to weather station placement are typical, because stations are located for convenience, access, and other practical concerns, such as the tremendous effort and cost required to maintain a year-round green field of grass. Similarly, evaporation

pans generally are not placed in uniform environmental settings, compromising transferability of measurements. McIlroy and Angus (1964) recommended a moist buffer of 20–50 m around an evaporation pan to avoid serious siting problems. This goal generally is not met for the same logistical reasons that the assumptions of  $ET_0$  computation generally are not met at most weather stations. Variability in maintenance, mounting, enclosures, and pan types also are complicating factors.

The impact of variations in station siting on site-to-site transfer value is probably more extreme for  $E_p$ , than for  $E_0$ , because of the strong feedback of the local surface cover on the measured  $E_p$ .  $E_p$  can be affected by energy inputs to the pan from surrounding areas, specifically, advected sensible heat from nearby drier areas, long-wave radiation from nearby warmer areas not subject to the degree of evaporative cooling occurring in the pan, and reflected radiation from nearby, usually more reflective, areas (Linacre, 1994). All of these energy inputs can change with variations in the local surface cover of the evaporation pan, implying that  $E_p$  measurements made in different settings are not comparable. In contrast, the prime determinant of measured  $ET_0$  is incoming solar radiation, which is unaffected by the local surface cover. However, the effects of local surface cover on other variables (air temperature, vapor-pressure deficit, and wind speed) within the  $ET_0$  computation (Eq. (8)) can introduce some error in estimating  $ET_0$ .

Year-to-year and seasonal variations in precipitation can be expected to provide good indications of variability in ET in the study area. This relation is evident through the relation of precipitation to cloud cover (and, therefore, incoming solar radiation and available energy) and to LAI and the strong role of solar radiation, available energy, and LAI in the calibrated, modified Priestley–Taylor model (Eqs. (10) and (12)) for  $ET_a$ . In other words, a year that is typical in precipitation is probably typical in ET. Precipitation in 2001 was generally representative of the long-term average conditions in seasonal distribution and annual total. The precipitation recorded at the NOAA weather station at the nearby city of Inverness was only about 37 mm below the long-term average of about 1360 mm. Therefore, the measured  $ET_a$  of 787 mm at the study site during 2001 can be regarded as representative of long-term, average

conditions. The measured precipitation at the study site during 2001 was 1191 mm, about 10% less than that measured at the nearby NOAA station for the same period. This discrepancy is about equal to the 10.2% discrepancy between these two rain gages over the 1996–2001 period of record at the weather station. Estimated long-term average ET constitutes about 66% of long-term annual precipitation at the study site.

The transfer of the relations for  $ET_a$  to other time periods is limited by the range of meteorological conditions encountered during the 19-month calibration period. The period chosen for this study was meteorologically typical for the area. However, the relations could vary during atypical conditions (e.g. very wet or very dry).

## 7. Conclusions

The Penman–Monteith (PM) and Priestley–Taylor (PT) models adequately reproduced 30-min values of actual evapotranspiration ( $ET_a$ ) from a nonirrigated pasture throughout a 19-month observation period. Both methods required calibration based on meteorological or vegetation data. The PT model, coupled with green-leaf area index (LAI) and solar radiation measurements, provided slightly improved  $ET_a$  predictions compared to the PM model. PM and PT models performed better at estimating daily  $ET_a$  than did either reference evapotranspiration ( $ET_0$ ) or pan evaporation ( $E_p$ ). However, the PM and PT data requirements of pasture-representative net radiation and soil heat flux may prove difficult based on typical siting of weather stations.

The  $ET_0$  vegetation coefficient was a simple function of LAI, whereas the  $E_p$  pan coefficient was a function of both LAI and  $E_p$ . The use of  $ET_0$  is preferred over  $E_p$  for several reasons.  $ET_0$  was a better predictor of  $ET_a$  than was  $E_p$ . Specifically, the standard error associated with the relation between  $ET_0$  and  $ET_a$  was about 28% lower than that between  $E_p$  and  $ET_a$ . The transferability of the inferred relations between  $ET_0$  and  $ET_a$  to other sites probably is better than that between  $E_p$  and  $ET_a$ . Also, precipitation corrections to measured  $E_p$  are subject to error. Finally, weather stations for measurement of  $ET_0$  are easily automated. The existing infrastructure

of weather stations available for the computation of  $ET_0$  offers great potential to also provide estimates of  $ET_a$ , which are needed for a variety of water management concerns. However, this potential can only be realized through identification of vegetation coefficient functions for a variety of environmental settings. This task can be completed in the manner exemplified for a single site in this study.

## Acknowledgements

Support for this study was provided by the US Geological Survey, Southwest Florida Water Management District, and NASA NIP Grant NAG5-10567. The contributions of Mark Condron (Southwest Florida Water Management District) in station construction and maintenance are gratefully acknowledged.

## References

- Allen, R.G., Periera, L.S., Raes, D., Smith, M., 1998. Crop Evapotranspiration: Guidelines for Computing Crop Requirements, Irrigation and Drainage Paper No. 56. FAO, Rome, Italy, p. 300.
- Asrar, G., Myneni, R.B., Kanemasu, E.T., 1989. Estimation of plant-canopy attributes from spectral reflectance measurement. In: Asrar, G. (Ed.), Theory and Applications of Optical Remote Sensing. Wiley, New York, pp. 252–296.
- Baldocchi, D.D., Hicks, B.B., Meyers, T.P., 1988. Measuring biosphere—atmosphere exchanges of biologically related gases with micrometeorological methods. *Ecology* 69 (5), 1331–1340.
- Baumgartner, A., Reichel, E., 1975. The World Water Balance. R. Oldenbourg-Verlag, München, Wien, pp. 1–179.
- Bidlake, W.R., 2002. Evapotranspiration and canopy resistance at an undeveloped prairie in a humid subtropical climate. *Journal of the American Water Resources Association* 38 (1), 197–211.
- Bowen, I.S., 1926. The ratio of heat losses by conduction and by evaporation from any water surface. *Physical Review*, 2nd series 26(6), 779–787.
- Brotzge, J.A., Crawford, K.C., 2003. Examination of the surface energy budget: a comparison of eddy correlation and Bowen ratio measurement systems. *Journal of Hydrometeorology* 4, 160–178.
- Brutsaert, W., 1982. Evaporation into the Atmosphere: Theory, History, and Applications. Kluwer, Boston, p. 299.
- Dale, R.F., Scheeringa, K., 1977. The effect of soil moisture on pan evaporation. *Agricultural Meteorology* 18, 463–474.

- Danish Hydraulic Institute, 1998. Anon., 1998. MIKE SHE User Guide and Technical Reference Manual. DHI Software, Denmark.
- Dingman, S.L., 1994. Physical Hydrology. Prentice-Hall, Upper Saddle River, NJ, p. 575.
- Dolman, A.J., Stewart, J.B., Cooper, J.D., 1988. Predicting forest transpiration from climatological data. *Agricultural and Forest Meteorology* 42, 339–353.
- Dugas, W.A., Fritschen, L.J., Gay, L.W., Held, A.A., Matthias, A.D., Reicosky, D.C., Steduto, P., Steiner, J.L., 1991. Bowen ratio, eddy correlation, and portable chamber measurements of sensible and latent heat flux over irrigated spring wheat. *Agricultural and Forest Meteorology* 56, 1–20.
- Dyer, A.J., 1961. Measurements of evaporation and heat transfer in the lower atmosphere by an automatic eddy-correlation technique. *Quarterly Journal of the Royal Meteorological Society* 87, 401–412.
- Eidenshink, J.C., 1992. The 1990 conterminous U.S. AVHRR data set. *Photogrammetric Engineering and Remote Sensing* 58 (6), 809–813.
- Farnsworth, R.K., Thompson, E.S., Peck, E.L., 1982. Evaporation atlas for the contiguous 48 United States. National Oceanic and Atmospheric Administration Technical Report NWS 33, 26, 4 sheets.
- Flint, A.L., Childs, S.W., 1991. Use of the Priestley–Taylor evaporation equation for soil water limited conditions in a small forest clearcut. *Agricultural and Forest Meteorology* 56, 247–260.
- German, E.R., 2000. Regional evaluation of evapotranspiration in the Everglades. US Geological Survey Water-Resources Investigations Report. 00-4217, p. 48.
- Goulden, M.L., Wofsy, S.C., Harden, J.W., Trumbore, S.E., Crill, P.M., Gower, S.T., Fires, T., Daubs, B.C., Fan, S.M., Sutton, D.J., Bassas, A., Munger, J.W., 1998. Sensitivity of boreal forest carbon balance to soil thaw. *Science* 279, 214–217.
- Harbaugh, A.W., Banta, E.R., Hill, M.C., McDonald, M.G. 2000. MODFLOW-2000, the US Geological Survey modular groundwater model—User guide to modularization concepts and the Ground-Water Flow Process. US Geological Survey Open-File Report. 00-92, p. 121.
- Jarvis, P.G., 1976. The interpretation of the variations in leaf water potential and stomatal conductance found in canopies in the field. *Philosophical Transactions of the Royal Society of London, Series B*, 593–610.
- Jensen, M.E., Burman, R.D., Allen, R.G. 1990. Evapotranspiration and Irrigation Water Requirements. ASCE Manuals and Reports on Engineering Practices No. 70, p. 352.
- Kohler, M.A., Nordenson, T.J., Fox, W.E., 1955. Evaporation from pans and lakes. US Weather Bureau Research Paper No. 38, p. 21.
- Kustas, W.P., Stannard, D.I., Allwine, K.J., 1996. Variability of surface energy flux partitioning during Washita'92: resulting effects on Penman–Monteith and Priestley–Taylor parameters. *Agricultural and Forest Meteorology* 82, 171–193.
- Linacre, E.T., 1994. Estimating US class a pan evaporation from few climate data. *Water International* 19, 5–14.
- Linacre, E.T., 2002. Ratio of lake to pan evaporation rates [cited March 2003] <http://www-das.uwyo.edu/~geerts/cwx/notes/chap04/eoep.html>
- Mahrt, L., 1998. Flux sampling errors for aircraft and towers. *Atmospheric Oceanic Technology* 15, 416–429.
- Martin, T.A., Brown, K.J., Cermak, J., Ceulemans, R., Kureca, J., Meinzer, F.C., Rombold, J.S., Sprugel, D.G., Hinckley, T.M., 1997. Crown conductance and tree stand transpiration in a second growth *Abies amabilis* forest. *Canadian Journal of Forest Resources* 27, 797–808.
- McIlroy, I.C., Angus, D.E., 1964. Grass, water, and soil evaporation at Aspendale. *Agricultural Meteorology* 1, 201–224.
- Monteith, J.L., 1965. Evaporation and environment, In: *Proceedings of the 19th Symposium of the Society for Experimental Biology*. Cambridge University Press, New York, NY pp. 205–233.
- Monteith, J.L., Unsworth, M.H., 1990. *Principles of Environmental Physics*, second ed. Edward Arnold, London, p. 291.
- Moore, C.J., 1976. Eddy flux measurements above a pine forest. *Quarterly Journal of the Royal Meteorological Society* 102, 913–918.
- Nemani, R., Running, S.W., 1989. Testing a theoretical climate-soil-leaf area hydrologic equilibrium of forests using satellite data and ecosystem simulation. *Agricultural and Forest Meteorology* 44, 245–260.
- Parton, W.J., Lauenroth, W.K., Smith, F.M., 1981. Water-loss from a shortgrass steppe. *Agricultural Meteorology* 24 (2), 97–109.
- Paulson, C.A., 1970. The mathematical representation of wind speed and temperature profiles in the unstable atmospheric surface layer. *Journal of Applied Meteorology* 9, 857–861.
- Penman, H.L., 1948. Natural evaporation from open water, bare soil, and grass. *Proceedings of the Royal Society, London A* 193, 120–146.
- Priestley, C.H.B., 1959. *Turbulent transfer in the lower atmosphere*. University of Chicago Press, Chicago, IL.
- Priestley, C.H.B., Taylor, R.J., 1972. On the assessment of surface heat flux and evaporation using large-scale parameters. *Monthly Weather Review* 100, 81–92.
- Rosset, M., Riedo, M., Grub, A., Geissmann, M., Fuhrer, J., 1997. Seasonal variation in radiation and energy balances of permanent pastures at different altitudes. *Agricultural and Forest Meteorology* 86, 245–258.
- Schotanus, P., Nieuwstadt, F.T.M., de Bruin, H.A.R., 1983. Temperature measurement with a sonic anemometer and its application to heat and moisture fluxes. *Boundary-Layer Meteorology* 26, 81–93.
- Schuepp, P.H., Leclerc, M.Y., MacPherson, J.I., Desjardins, R.L., 1990. Footprint prediction of scalar fluxes from analytical solution of the diffusion equation. *Boundary-Layer Meteorology* 50, 355–373.
- Slatyer, R.O., McIlroy, I.C., 1961. *Practical microclimatology*. CSIRO, Melbourne, Australia.
- Stannard, D.I., 1993. Comparison of Penman–Monteith Shuttleworth–Wallace, and modified Priestley–Taylor evapotranspiration models for wildland vegetation in semiarid rangeland. *Water Resources Research* 29 (5), 1379–1392.

- Stewart, J.B., 1988. Modeling surface conductance of pine forest. *Agricultural and Forest Meteorology* 43, 19–35.
- Stewart, J.B., Gay, L.W., 1989. Preliminary modeling of transpiration from the FIFE site in Kansas. *Agricultural and Forest Meteorology* 48, 305–310.
- Sumner, D.M., 1996. Evapotranspiration from successional vegetation in a deforested area of the Lake Wales Ridge, Florida. US Geological Survey Water-Resources Investigations Report. 96-4244, p. 38.
- Sumner, D.M., 2001. Evapotranspiration from a cypress and pine forest subjected to natural fires in Volusia County, Florida, 1998–1999, US Geological Survey Water-Resources Investigations Report. 01-4245, p. 55.
- Swancar, Amy, Lee, T.M., O'Hare, T.M., 2000. Hydrogeologic setting, water budget, and preliminary analysis of ground-water exchange at Lake Starr, a seepage lake in Polk County, Florida, Water-Resources Investigations Report 00-4030, p. 65.
- Tanner, B.D., Greene, J.P., 1989. Measurements of sensible heat flux and water vapor fluxes using eddy correlation methods. Final report to US Army Dugway Proving Grounds, DAAD 09-87, D-0088.
- Tanner, C.B., Thurtell, G.W., 1969. Anemoclinometer measurements of Reynolds stress and heat transport in the atmospheric boundary layer. US Army Electronics Command, Atmospheric Sciences Laboratory, Fort Huachuca, Arizona, TR ECOM 66-G22-F, Reports Control Symbol OSD-1366, April 1969, p. 10.
- Twine, T.E., Kustas, W.P., Norman, J.M., Cook, D.R., Houser, P.R., Meyers, T.P., Prueger, J.H., Starks, P.J., Wesely, M.L., 2000. Correcting eddy-covariance flux underestimates over a grassland. *Agricultural and Forest Meteorology* 103, 279–300.
- US Army Corps of Engineers, 2000. Hydrologic Modeling System HEC-HMS—Technical Reference Manual. US Army COE Hydrologic Engineering Center, Davis, CA, 149p.
- Vogelmann, J.E., Howard, S.M., Yang, L., Larson, C.R., Wylie, B.K., van Driel, N., 2001. Completion of the 1990s National Land cover data set for the conterminous United States from landsat thematic mapper data and ancillary data sources. *Photogrammetric Engineering and Remote Sensing* 67, 650–652.
- Walter, I.A., Allen, R.G., Elliott, R., Mecham, B., Jensen, M.E., Itenfisu, D., Howell, T.A., Snyder, R., Brown, P., Echings, S., Spofford, T., Hattendorf, M., Cuenca, R.H., Right, J.L., Martin, D., 2000. ASCE standardized reference evapotranspiration equation, in: Evans, R.G., Benham, B.L., Troien, T.P. (Eds.), *Proceedings of the National Irrigation Symposium*, ASAE, Nov. 14–16, Phoenix, AZ, pp. 209–215.
- Wang, J., Rich, P.M., Price, K.P., 2003. Temporal responses of NDVI to precipitation and temperature in the central great plains, USA. *International Journal of Remote Sensing* 24, 2345–2364.
- Webb, E.K., Pearman, G.I., Leuning, R., 1980. Correction of flux measurements for density effects due to heat and water vapour transfer. *Quarterly Journal of the Royal Meteorological Society* 106, 85–100.
- Wright, I.R., Manzi, A.O., da Rocha, H.R., 1995. Surface conductance of Amazonian pasture: model application and calibration for canopy climate. *Agricultural and Forest Meteorology* 75, 51–70.